Assimilating TOVS Humidity into the GEOS-2 Data Assimilation System

MINGHANG CHEN,* RICHARD B. ROOD, AND JOANNA JOINER
NASA/Goddard Space Flight Center, Greenbelt, Maryland

(Manuscript received 15 September 1998, in final form 28 December 1998)

ABSTRACT

The humidity data retrieved from the TIROS Operational Vertical Sounder (TOVS) measurements is assimilated into the Goddard Earth Observing System (GEOS) data assimilation system. The study focuses on the impact of the TOVS humidity on assimilated humidity, precipitation, clouds, and radiation. The GEOS assimilation system utilizes the TOVS humidity effectively at levels below 300 mb, while the net impact on the 300-mb humidity is much less. It has been demonstrated that the impact results from direct and indirect effects. The direct effect is the analysis increment introduced by the humidity data, which draws the assimilated humidity toward the data. The indirect effect is realized through the interactions of humidity with physical processes, mainly with moist convection. The indirect effect is often opposite to the direct effect in the current assimilation system. The direct effect is dominant in the lower and middle troposphere while in the upper troposphere the indirect effect is more important. The impact of the TOVS humidity on the GEOS precipitation, clouds, and radiation is also significant due to strong interactions with convection and other physical processes. There is clear evidence indicating that tuning of physical parameterizations explicitly in the data assimilation mode is necessary for optimal use of the TOVS data in the assimilation system.

1. Introduction

Water vapor feedback is an important issue for the understanding of climate change. The climate sensitivity parameter, defined by Cess et al. (1990) as the ratio of global-mean surface temperature change to direct radiative forcing, is greatly enhanced by water vapor feedback. Cess et al. (1990) have shown that water vapor feedback enhances by 70% the clear-sky climate sensitivity in 19 general circulation models (GCMs). Although there is a consensus on the positive impact of water vapor feedback, it is difficult to quantitatively verify the water vapor feedback simulated by GCMs due to the lack of reliable observations of water vapor, especially in the upper troposphere (Starr and Melfi 1991).

Sun and Held (1996) have compared humidity–temperature relationships in the Tropics from rawinsonde data and a GCM simulation. They found that the link between humidity and temperature is significantly stronger in the GCM simulation than in rawinsonde observations. It is not clear, however, how much of this discrepancy is due to errors in the model, because there are large uncertainties in rawinsonde data (Elliot and Gaffen 1991; Starr and Melfi 1991). There are several factors contributing to uncertainties in rawinsonde data. First, inadequate horizontal coverage and resolution, especially over the vast oceanic regions, is a major problem since water vapor changes rapidly in space. Second, uncertain data quality arises from significant environment-dependent sensor errors and variations in sensor types and reporting practices. The third factor is inadequate vertical resolution in the middle troposphere and very few data in the upper troposphere.

Limitations and uncertainties in rawinsonde humidity observations seriously undermine the quality of humidity fields from recent reanalyses with global data assimilation systems (e.g., Schubert et al. 1993; Kalnay et al. 1996) that use rawinsonde measurements as the only data source for humidity analysis. Recent progress in estimation of water vapor from satellite measurements (e.g., Schmetz and Turpeinen 1988; Rind et al. 1993; Read et al. 1995; Susskind et al. 1997) has provided new opportunities for better representation of humidity in a data assimilation system (DAS) (e.g., McNally and Vesperini 1996). There are two basic approaches to assimilating satellite humidity information into a DAS. The first approach is to assimilate humidity data retrieved from radiances measured by satellite instruments. Humidity retrieval may be done by a satellite data producer independent of the DAS. Since humidity

* Additional affiliation: General Sciences Corporation, a subsidiary of Science Applications International Corporation, Beltsville, Maryland.

Corresponding author address: Dr. Minghang Chen, NASA/Goddard Space Flight Center, Code 910.3, Greenbelt, MD 20771.
E-mail: mchen@dao.gsfc.nasa.gov

is a model prognostic variable, it is straightforward to assimilate satellite-retrieved humidity data. The second approach is to assimilate radiance measurements directly into a DAS. This approach requires an observation operator built into the DAS to transform model variables into radiances. Direct radiance assimilation is theoretically superior to retrieval assimilation because necessary assumptions made for observational error statistics are more justified in radiance assimilation than in retrieval assimilation (Eyre et al. 1993). For future high-spectral resolution instruments with large number of channels, Joiner and da Silva (1998) have proposed efficient alternative methods.

In this study we assimilate humidity information from the TIROS Operational Vertical Sounder (TOVS) into the Goddard Earth Observing System (GEOS) data assimilation system. We will focus on the impact of the TOVS humidity data on assimilated humidity and the impact on precipitation, clouds, and radiation, which are closely related to humidity or interact strongly with humidity. As a first step, we use the first approach discussed above to assimilate TOVS humidity; that is, we assimilate the retrieved humidity.

Sections 2 and 3 give brief descriptions of the TOVS humidity data and the GEOS DAS, respectively. Section 4 describes the impact on the GEOS humidity fields. Section 5 shows the impact on precipitation, clouds, and radiation. Discussion and conclusions are given in section 6.

2. TOVS humidity

The TOVS humidity data assimilated in the present study is from the TOVS pathfinder path A dataset (Susskind et al. 1997). The TOVS humidity is retrieved from radiance measured by the second version of the High-Resolution Infrared Radiation Sounder (HIRS-2) on the National Oceanic and Atmospheric Administration (NOAA) polar-orbiting satellites (Smith et al. 1979). The retrieval methodology used is similar to that described in Reuter et al. (1988) and Susskind et al. (1984).

The retrieval system uses the first guess of temperature and humidity profiles produced by the first version of the GEOS DAS (GEOS-1; Takacs et al. 1994; Pfaendtner et al. 1995) at the resolution of 4° lat × 5° long. The humidity retrieval is performed subsequent to the temperature retrieval and only when the temperature retrieval succeeds. The humidity retrieval uses radiances of HIRS-2 channels 8 and 10–12. Channel 10 is sensitive to water vapor in the lower troposphere while channels 11 and 12 are sensitive to water vapor in the middle and upper troposphere (Smith et al. 1979; McNally and Vesperini 1996). After the retrieved humidity profiles are generated, a systematic error correction methodology is used to modify the retrieved humidity profiles. The systematic error correction utilizes collocated radiosonde reports. The correction has indirect effects in regions with no radiosonde reports besides direct effects in regions with radiosonde reports.

Retrieved specific humidity is available at six pressure levels (1000, 850, 700, 500, 400, and 300 mb). Susskind et al. (1997) have shown that the TOVS total precipitable water (TPW) from *NOAA-11* for December 1989 agrees well with the independent TPW estimated from the Special Sensor Microwave/Imager (SSM/I; Wentz 1994). The difference between the two estimations, globally averaged over the oceans, is 0.24 kg m^{-2} with a dry bias of the TOVS TPW relative to the SSM/I TPW. The mean value of the SSM/I TPW is 27.5 kg m^{-2}. The dry bias of the TOVS TPW is, at least partly, related to the fact that the TOVS retrieval is not valid for overcast or precipitating regions. Additional comparison of TPW from TOVS and SSM/I is given in section 4.

The instantaneous TOVS humidity is used in the present assimilation experiment. Due to high volume of the input data, a thinning method is used to reduce the data volume. The instantaneous TOVS humidity data is spatially averaged for each grid box with the GEOS DAS resolution of 2° lat × 2.5° long before it is read in by the assimilation system. For a typical day, the number of grid boxes with valid TOVS humidity is about 20 times larger than that of rawinsonde humidity observations. The assimilation system does quality controls (both a background check and a buddy check) on the TOVS humidity data. Generally, about 2% of the TOVS data is rejected by quality controls.

3. Assimilation system and experiments

The GEOS data assimilation system is being developed to support NASA's Earth Observing System (EOS) and to provide the research community with reanalysis data with new data types incorporated, especially those observed from EOS. The first frozen version of the GEOS DAS, GEOS-1, has been used for the NASA multiyear reanalysis (Schubert et al. 1993). The system used in the present study is a current version of the second generation GEOS system (GEOS-2). GEOS-2 has been developed based on GEOS-1 with a special effort to address problems and shortcomings discovered in the GEOS-1 reanalysis (Schubert and Rood 1995). GEOS-2 will be used for the support of the EOS AM-1 launch. A detailed description of GEOS-2 is given in DAO (1996). The following gives a brief description of GEOS-2.

The GEOS-2 DAS consists of the GEOS-2 GCM and the GEOS-2 Physical-space Statistical Analysis System (PSAS). The GEOS-2 GCM uses version 2 of the Aries/GEOS dynamical core (Suarez and Takacs 1995), which is a fourth-order energy and potential enstrophy conserving scheme. The turbulence parameterization in the GEOS-2 GCM consists of components that handle vertical diffusion and surface fluxes of heat, moisture, and momentum (Helfand and Labraga 1988). The relaxed

Arakawa–Schubert (RAS) scheme (Moorthi and Suarez 1992), which is a simple and efficient implementation of the Arakawa–Schubert scheme (Arakawa and Schubert 1974), is used to parameterize moist convection. The model also includes a parameterization of reevaporation of falling rain (Sud and Molod 1988). The scheme accounts for rainfall intensity, drop size distribution, and environmental temperature, pressure, and relative humidity. Convective and large-scale (layered) clouds are diagnosed in the parameterizations of moist convection and large-scale condensation. Convective cloud cover is proportional to detrained liquid water amount given by RAS, and large-scale cloudiness is calculated with a scheme similar to Slingo (1987). The longwave and shortwave radiation schemes are described by Chou and Suarez (1994) and Chou (1992), respectively. Cloud optical thickness is specified as a function of cloud type and cloud water content (DAO 1996). The GEOS-2 GCM also has a gravity wave drag scheme (Zhou et al. 1996).

The GEOS-2 PSAS is an entirely different algorithm than that used in GEOS-1. It solves analysis equations globally. This eliminates the local approximation and data selection of the optimal interpolation (OI) scheme used in the GEOS-1 system (Pfaendtner et al. 1995). In this respect, PSAS is comparable to the global variational spectral analysis systems that have recently been implemented at the National Centers for Environmental Prediction (Parrish and Derber 1992) and the European Centre for Medium-Range Weather Forecasts (ECMWF; Courtier et al. 1998). But PSAS, unlike spectral analysis schemes, works directly in physical space. PSAS performs a large part of its calculations in observation space, also unlike operational spectral analysis schemes, which operate in state space. This results in computational savings, since the dimension of the observation space is currently an order of magnitude smaller than that of the analysis state. The computational efficiency of spectral analysis schemes arises from an assumption that horizontal forecast error covariances or correlations are isotropic, that is, diagonal in spectral space, an assumption that is not necessary in the PSAS algorithm.

Another change from GEOS-1 to GEOS-2, especially important for upper-tropospheric humidity (UTH), is the calculation of saturation humidity. In GEOS-1, saturation humidity is calculated with respect to (wrt) liquid regardless of temperature. In GEOS-2, saturation humidity is calculated wrt ice when temperature is below $-40°$C and a linear combination of two calculations (one wrt liquid and one wrt ice) for temperature between $0°$ and $-40°$C. Chen et al. (1998) have shown that this change significantly reduces UTH.

The GEOS-2 DAS uses the GEOS-2 GCM with horizontal resolution of $2°$ lat $\times$ $2.5°$ long and 70 sigma levels and the GEOS-2 PSAS with the same horizontal resolution but 18 pressure levels (1000, 850, 700, 500, 400, 300, 250, 200, 150, 100, 70, 50, 30, 10, 7, 5, 1, and 0.4 mb) and sea level. To produce assimilations, analysis increments computed by PSAS are integrated into the GEOS-2 GCM with an approach called the incremental analysis update (Bloom et al. 1996). The moisture analysis is performed only at the lowest six levels (300 mb and below). In the standard or control assimilation (CTL) the system uses only rawinsonde humidity observations. For the experimental assimilation (EXP), however, the system uses the TOVS retrieved specific humidity in addition to rawinsonde observations. Both assimilations were integrated from 15 December 1991 through 31 January 1992. Monthly means for January 1992 are shown in this paper. In next sections we will show differences between the two assimilations to illustrate the impact of the inclusion of TOVS humidity on assimilated fields.

4. Impact on humidity

We use the latest version SSM/I TPW, an independent dataset, for the TPW validation of the assimilations. SSM/I contains more microwave channels than TOVS. These channels provide enhanced information about TPW over the oceans because the low microwave emissivity of the ocean surface provides a cold background as compared with emission from atmospheric water vapor. Therefore SSM/I TPW is expected to be more accurate than that from TOVS. First, we compare the TOVS TPW with SSM/I. Figures 1a and 1b show TPW from SSM/I and TOVS, respectively. In the Tropics the TOVS TPW is in good agreement with SSM/I. However, the high TPW band with values greater than 36 kg m^{-2} is latitudinally wider in TOVS than in SSM/I. The sharp gradient of TPW in the Tropics is weaker in TOVS than in SSM/I. Another difference is that the bulges in the northeastern Pacific and the northeastern Atlantic are weaker in TOVS than in SSM/I. The differences between Figs. 1a and 1b (not shown) indicate that the TOVS TPW has small dry biases in cloudy regions and wet biases in clear-sky regions with magnitudes of 2–8 kg m^{-2}.

We next compare TPW from the two assimilations with SSM/I. Figure 1c shows the TPW differences between the CTL assimilation and SSM/I. The CTL assimilation has large overestimation of TPW in most tropical oceanic regions to the north of the equator and in the central equatorial Pacific where the largest TPW is located in CTL. Figure 1d shows the differences between the EXP assimilation (with inclusion of the TOVS humidity) and SSM/I. It is encouraging that large tropical wet biases found in CTL are significantly reduced in EXP. Also, plots with a finer color scale (not shown in this paper) indicate an improvement of TPW over the winter storm tracks in the North Pacific and the North Atlantic. In some regions of the Southern Hemisphere (SH), however, biases are slightly larger in EXP than in CTL. This is caused by the wet biases of the TOVS TPW relative to the SSM/I TPW in those regions.

It is useful to examine the humidity impact in the

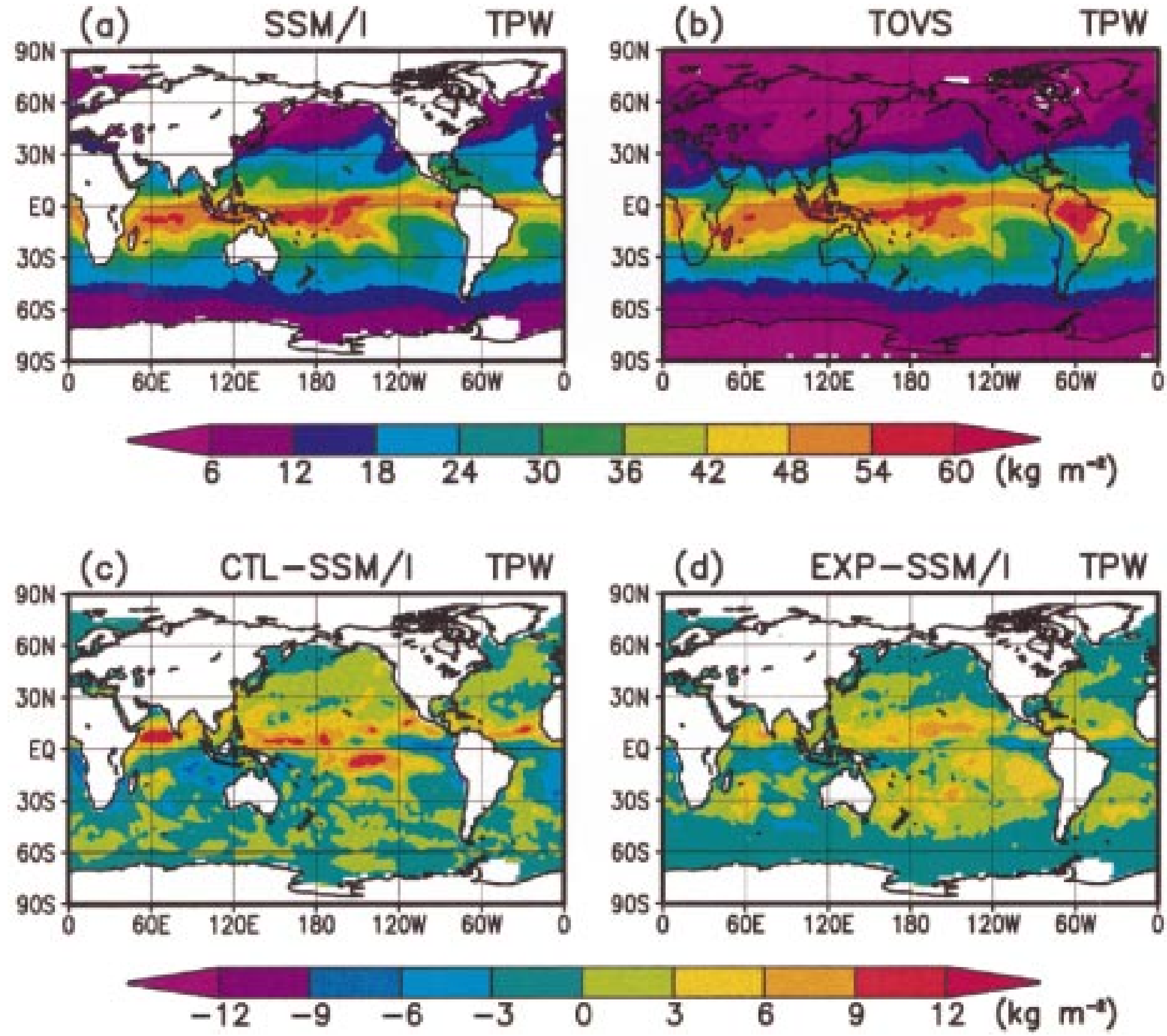

FIG. 1. Total precipitable water from (a) SSM/I and (b) TOVS; and differences between the assimilations and SSM/I (c) CTL minus SSM/I and (d) EXP minus SSM/I.

lower, middle, and upper troposphere separately because accurate assimilations of moisture vertical structures are very important. Due to the lack of accurate humidity data with global coverage and vertical structure, it is difficult to objectively validate changes in humidity at various levels. Here we focus on the comparison between the assimilations and the TOVS humidity data. This is not an independent validation of the TOVS data impact, but rather an investigation to see whether the data is rejected by the assimilation system. By rejected, we mean that the model physics may try to remove humidity changes introduced by the data.

Figure 2a shows the CTL humidity at 850 mb. A large humidity band exists along the equator with maximum values over deep convection centers along the intertropical convergence zone (ITCZ). Figure 2b shows humidity differences between CTL and TOVS. In the SH low latitudes (0°–35°) except for the central tropical Pacific, the CTL humidity is significantly drier than the TOVS humidity. Due to this dry bias in CTL, the TOVS humidity data should have a moistening impact in EXP over those regions. Figure 2c shows the humidity analysis increment in EXP. The analysis increment is the forcing term introduced by the humidity data due to the difference between the model's first guess and the data. Since there are few rawinsonde humidity observations in the Tropics and SH (Schubert et al. 1995), large positive analysis increments in Fig. 2c are due mainly to the TOVS humidity data. As a result, the assimilated humidity from EXP should be much closer to the TOVS humidity. Figure 2d shows the differences between EXP and TOVS. The large biases found in CTL, both positive

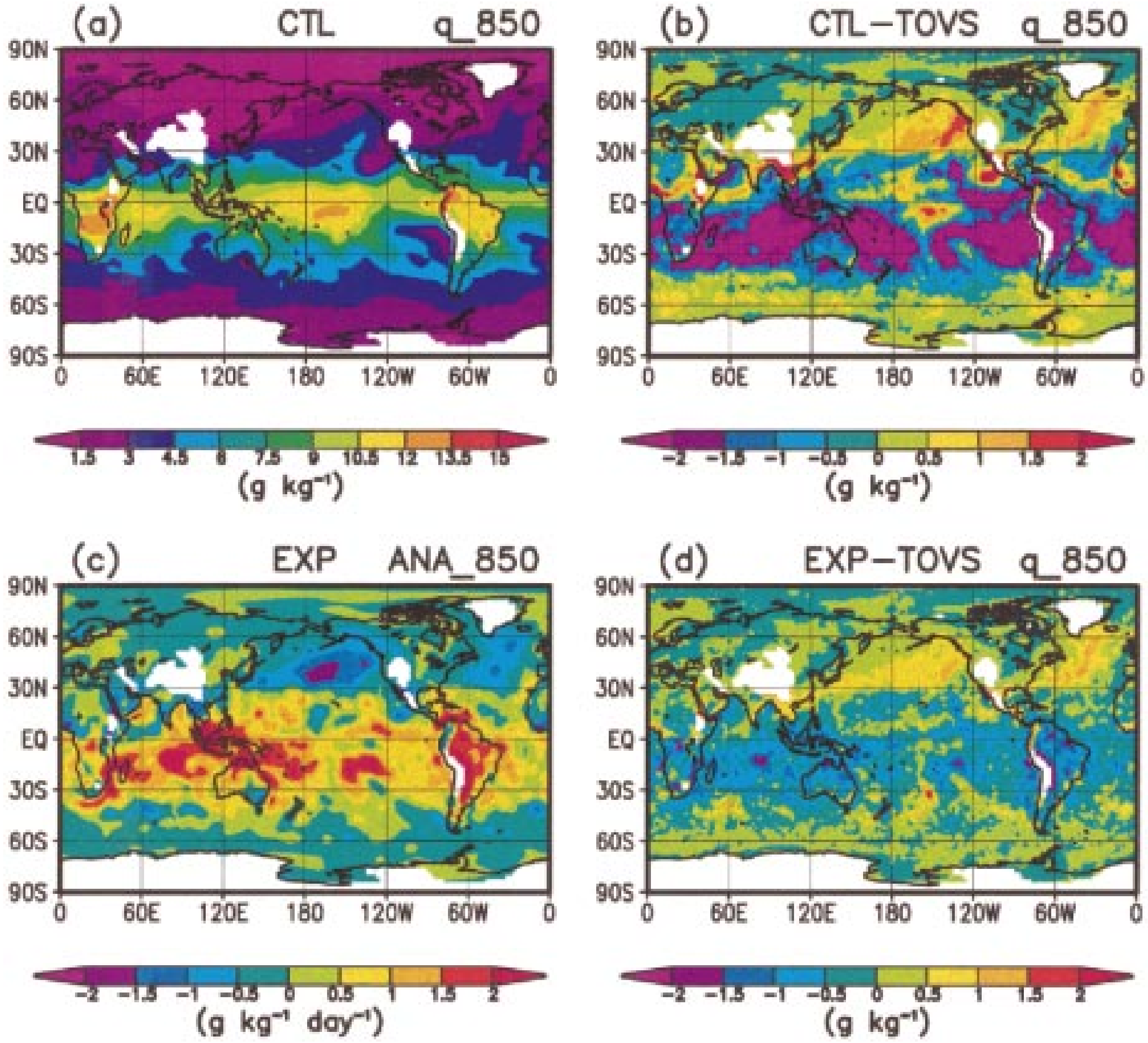

FIG. 2. (a) Specific humidity at 850 mb from CTL, (b) differences in humidity between CTL and TOVS, (c) analysis increments of humidity in EXP, and (d) differences in humidity between EXP and TOVS.

and negative, are largely reduced. It is clear that the GEOS assimilation system uses the TOVS humidity data very effectively at this level.

Figure 3a shows the CTL specific humidity at 500 mb. The largest humidity at this level exists in the central equatorial Pacific. This is caused by the eastward shift of strong deep convection associated with the sea surface temperature (SST) anomaly that occured during the El Niño event (Kousky 1993). The CTL humidity is greater than the TOVS humidity in almost all oceanic regions (Fig. 3b). The differences are particularly large in low-latitude oceanic areas. Thus, inclusion of the TOVS humidity data should reduce the humidity at 500 mb. Figure 3c shows the analysis increments of humidity in EXP. The large negative increments in Fig. 3c correspond to the positive differences seen in Fig. 3b and vice versa. The humidity differences between EXP and TOVS (Fig. 3d) are much less than those between CTL and TOVS (Fig. 3b). However, the EXP humidity in some regions is still significantly larger than TOVS.

Figure 4a shows the CTL humidity at 300 mb. High humidity is closely associated with deep convection along the ITCZ. Compared with the TOVS humidity, the CTL humidity is much higher over most regions in low latitudes (Fig. 4b). In the central tropical Pacific and the tropical Indian Ocean, the CTL humidity is two to three times as large as the TOVS humidity. Inclusion of the TOVS data gives large negative analysis increments in the Tropics in the EXP assimilation (Fig. 4c). Figure 4d shows the differences between EXP and TOVS. Even though the negative analysis increments due to the TOVS data in EXP are very strong, the wet

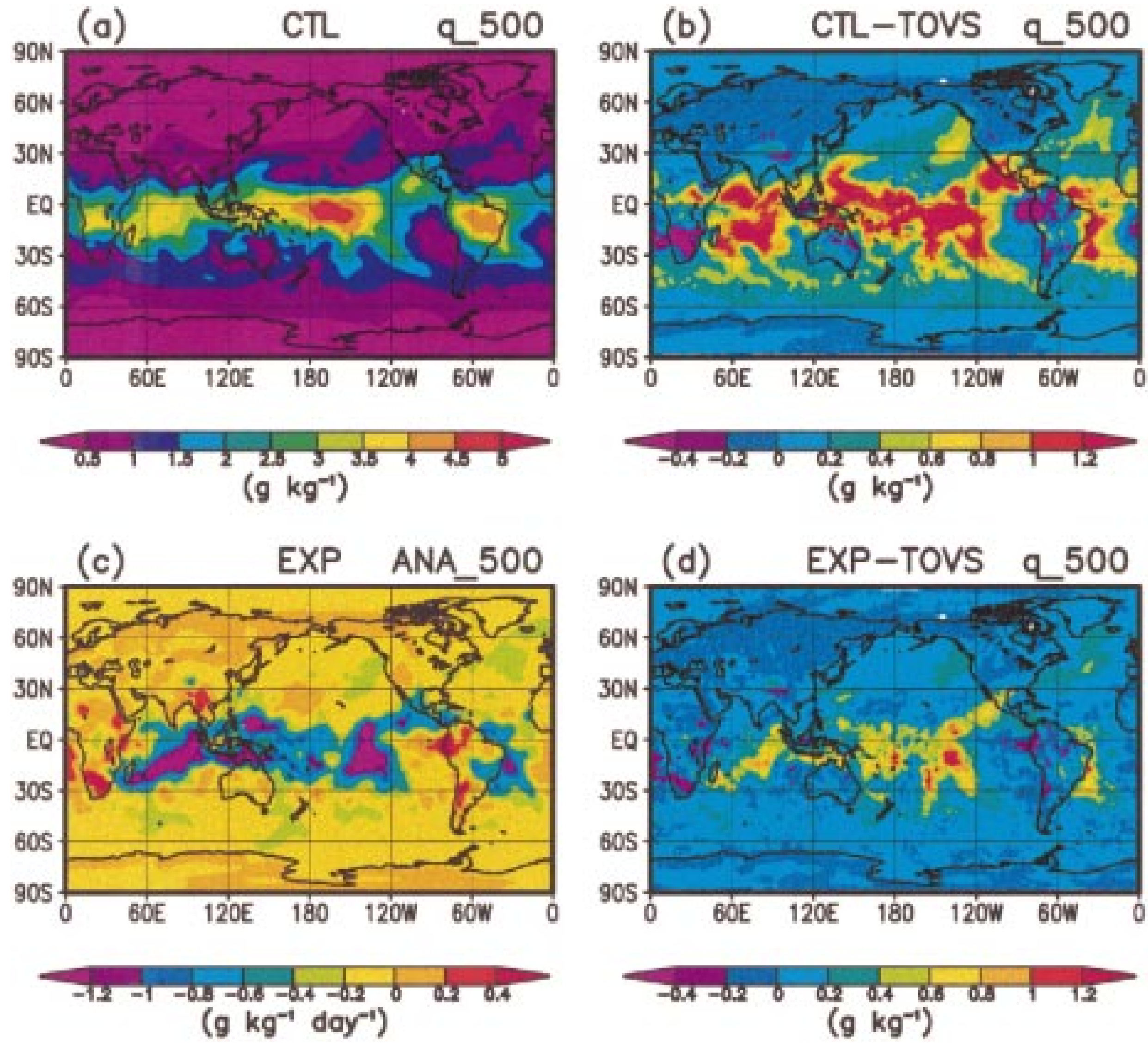

FIG. 3. (a) Specific humidity at 500 mb from CTL, (b) differences in humidity between CTL and TOVS, (c) analysis increments of humidity in EXP, and (d) differences in humidity between EXP and TOVS.

biases in the central tropical Pacific and the tropical Indian Ocean are only slightly reduced in EXP. Furthermore, the wet biases in some regions such as southern Africa and South America increase (see Fig. 5b for details). This implies the analysis increment is compensated or even dominated by opposite changes in other moisture forcing terms in GEOS-2. Since tropical deep convection has a predominant effect on tropical upper tropospheric humidity (Chen et al. 1998, 1999), the opposite (moistening) impact should result mainly from changes in deep convection.

We use vertical velocity at 400 mb as an indication of the strength of tropical deep convection because ascending motion is strongest around 400 mb in the Tropics (Schubert et al. 1995). Figure 5a shows differences between the two assimilations in vertical velocity ω at 400 mb ($\omega = dp/dt$, where p is the pressure and t is the time). Negative differences in ω indicate enhanced ascending motion. It is clear that deep convection in the EXP assimilation is stronger than in CTL in southern Africa, South America, and some other regions in the Tropics. In the central tropical Pacific just to the south of the equator, deep convection in EXP is weaker than in CTL. Figure 5b shows differences in humidity at 300 mb between the two assimilations. There is a good relationship between negative ω differences and positive humidity differences due to moistening effect of enhanced deep convection. This suggests that the moistening effect of enhanced deep convection is dominant over the negative humidity analysis increment shown in Fig. 4c. On the other hand, there is no corresponding negative humidity difference with similar spatial cov-

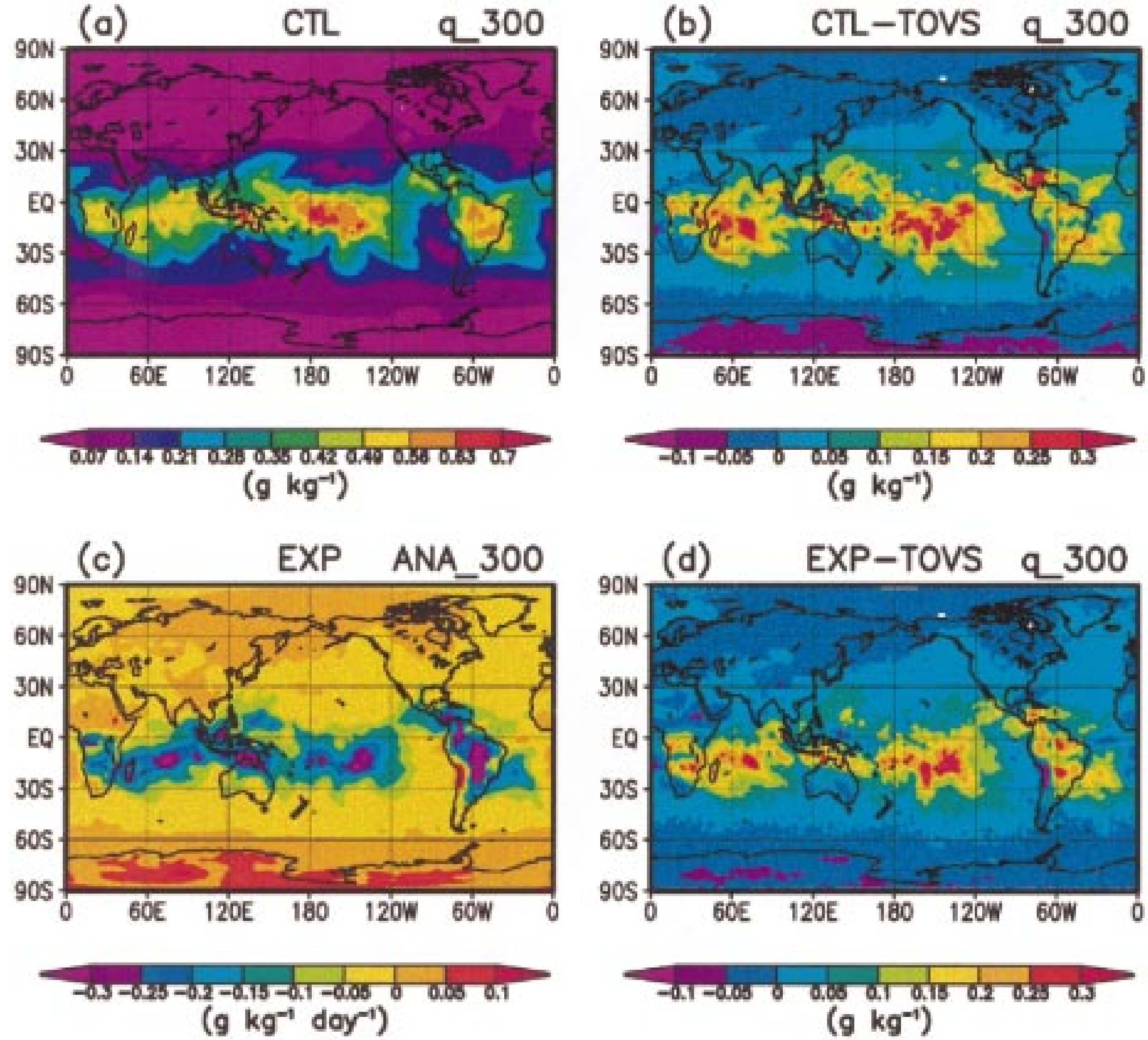

FIG. 4. (a) Specific humidity at 300 mb from CTL, (b) differences in humidity between CTL and TOVS, (c) analysis increments of humidity in EXP, and (d) differences in humidity between EXP and TOVS.

erage in the central tropical Pacific where a large positive ω difference exists. This is unexpected because both the reduced convection and the negative analysis increment in the region (Fig. 4c) have drying effects. It suggests a role of other mechanisms, such as large-scale advection and subgrid mixing, in redistribution of upper-tropospheric water vapor.

It has been demonstrated that assimilating the TOVS humidity data into GEOS-2 has a profound impact on convection, which in turn has a large effect on humidity. This effect due to the interactions with convection is here referred to as the indirect effect. For the lower and middle troposphere, the direct effect (the analysis increment) of the TOVS humidity data on the assimilated humidity is dominant over the indirect effect. For the upper troposphere, however, the indirect effect becomes more important.

5. Impact on precipitation, clouds, and radiation

For the evaluation of precipitation we use the precipitation dataset from the Global Precipitation Climatology Project (GPCP; Huffman et al. 1997). The GPCP precipitation is a combination of rain gauge measurements and satellite estimations from both microwave (SSM/I) and infrared (various geostationary satellites) measurements. The dataset also includes the estimated errors, which vary with space and time. For January 1992, the relative errors are 15%–25% in the Tropics and 25%–30% over the winter storm tracks.

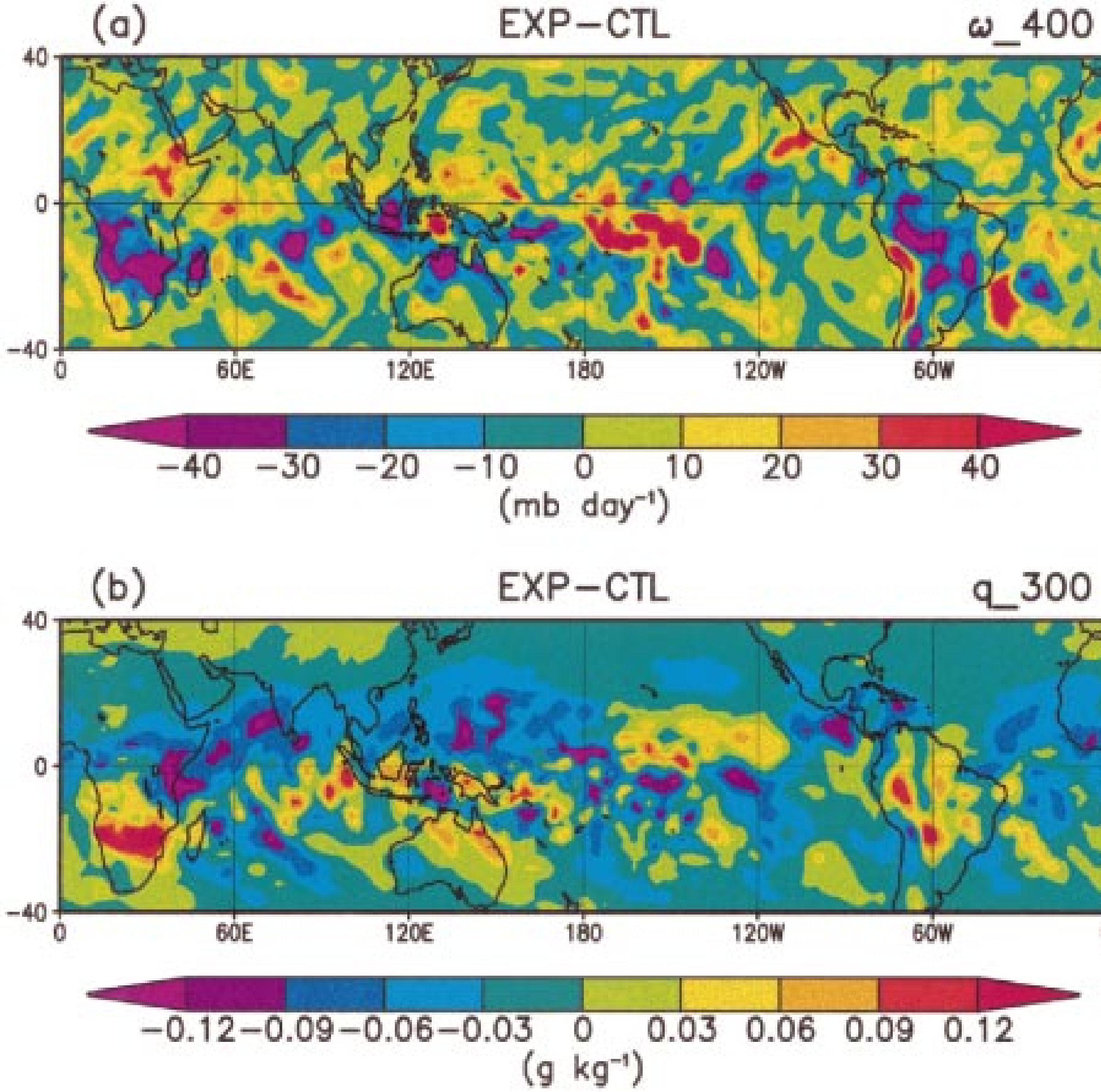

FIG. 5. Differences in (a) vertical velocity ω at 400 mb and (b) specific humidity at 300 mb between EXP and CTL.

The precipitation from EXP and CTL is shown in Fig. 6 with the GPCP estimation. The two assimilations have heavy precipitation in convective regions along the ITCZ, which is consistent with GPCP. Precipitation along the ITCZ is generally enhanced in EXP as compared with CTL (Fig. 6d). The largest enhancement is found in southern Africa and South America. In the central tropical Pacific, however, precipitation is weaker in EXP. The differences in tropical precipitation are consistent with the changes in convection indicated by the 400 mb ω field shown in Fig. 5a. Compared to GPCP, these changes indicate general deterioration of precipitation in the EXP assimilation. As examples, precipitation in the central tropical Pacific is already too weak in CTL, but even weaker in EXP. In southern Africa and South America, precipitation is about right in CTL while too strong in EXP. In the extratropics, large precipitation associated with the winter storm tracks in the North Pacific and the North Atlantic is much reduced in EXP, which is another major deterioration.

Assimilation of the TOVS humidity into GEOS-2 gives better moisture fields (TPW and specific humidity in the lower and middle troposphere), but not a better precipitation field. A similar result was found by McNally and Vesperini (1996) when they assimilated the TOVS radiance of the water vapor channels into the ECMWF assimilation system with a one-dimensional variational analysis scheme (1DVAR). They found that

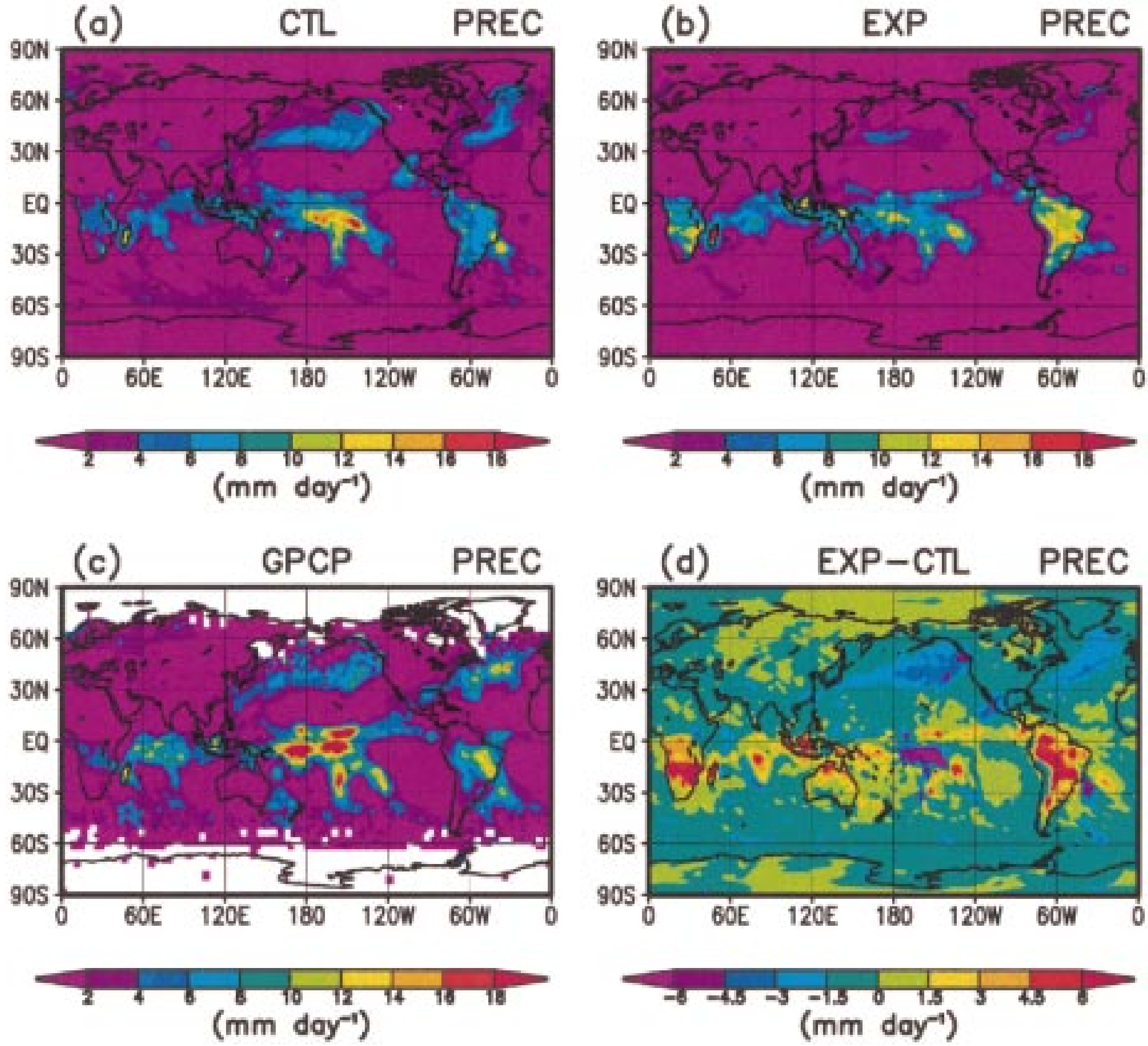

FIG. 6. Precipitation from (a) CTL, (b) EXP, and (c) GPCP; and differences (d) between EXP and CTL.

the TOVS radiance assimilation improves the TPW field significantly, but has no clear positive impact on the precipitation field. The inconsistency implies complicated interactions between humidity and parameterized physics in an assimilation system. Usually there is extensive tuning of physical parameterizations involved during the development of an assimilation system. When new types of observations become available, it might be necessary to retune the system to achieve overall improvements on assimilations with new observations included. A further discussion on this issue is given in the next section.

Figure 7 shows the total cloud amount from the two assimilations and the International Satellite Cloud Climatology Project (ISCCP; Rossow and Schiffer 1991). The cloud amount along the ITCZ is generally greater in EXP than in CTL (Fig. 7d), which is consistent with the changes in deep convection. In the subtropics of the Northern Hemisphere (NH) the EXP assimilation has less cloud amount than the CTL assimilation. The cloud amount is also reduced over the NH winter storm tracks and the vast oceanic regions in the SH midlatitudes. In the high latitudes of both hemispheres, however, the cloud amount is significantly greater in EXP than in CTL. These changes in the total cloud amount generally make EXP farther away from ISCCP. This is not surprising after we have seen the deterioration in the precipitation field when the TOVS humidity data is included. The changes in clouds indicate strong interactions between humidity and clouds in convective regions (the ITCZ and the winter storm tracks) and nonconvective regions (the NH subtropics, the SH midlatitudes,

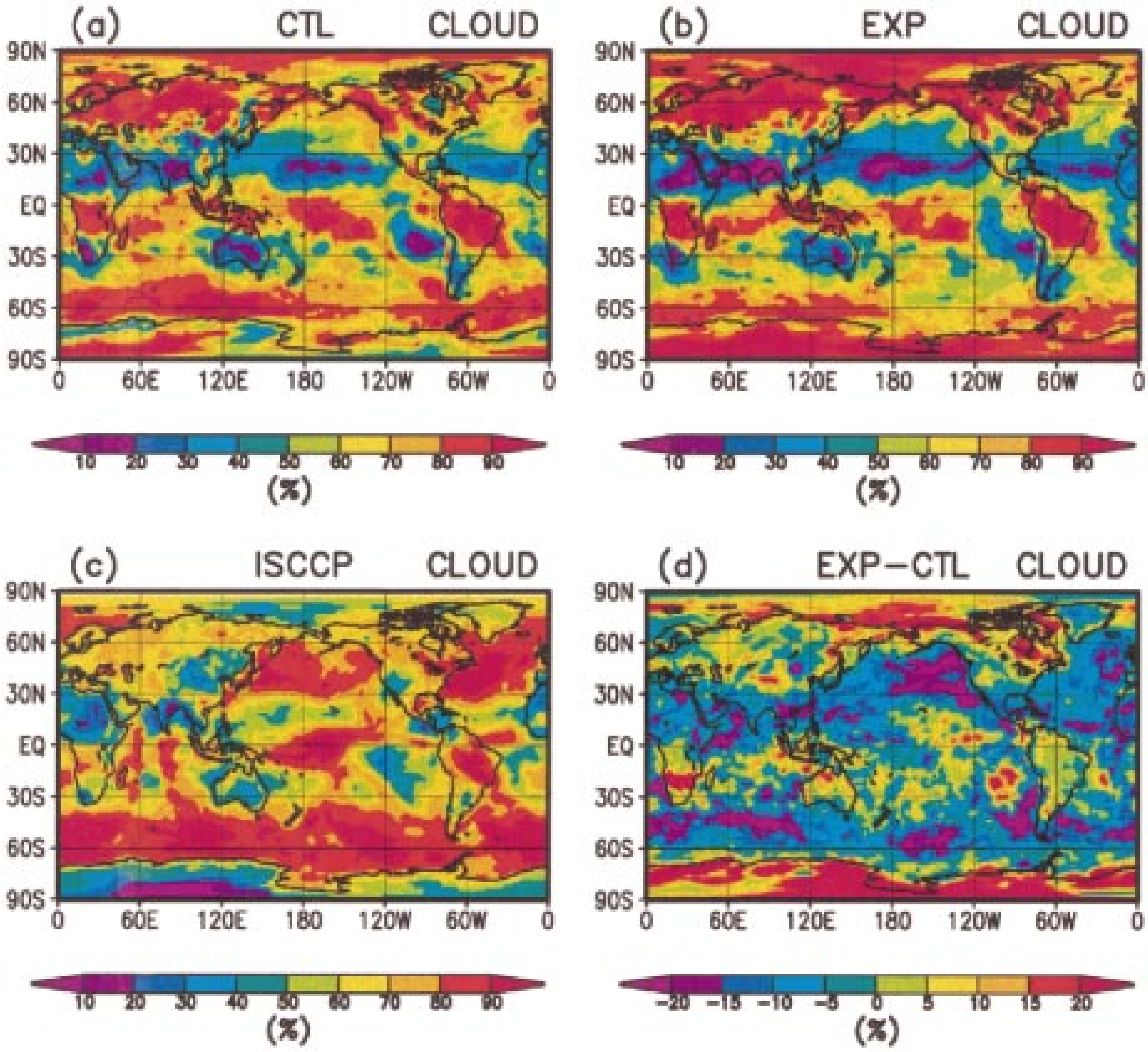

FIG. 7. Total cloud amount from (a) CTL, (b) EXP, and (c) ISCCP; and differences (d) between EXP and CTL.

and the high latitudes of both hemispheres). Large changes in clouds have enormous impacts on radiation budget in the atmosphere and on the surface.

Figure 8a shows differences in the outgoing longwave radiation (OLR) at the top of the atmosphere (TOA) between the two assimilations. Negative (positive) differences in OLR correspond well to positive (negative) difference in the cloud amount (Fig. 7d) due to the greenhouse effect of clouds. The greenhouse effect of clouds depends on cloud amount, cloud height and temperature, and cloud radiative properties. Changes in humidity also have an effect on OLR, which is important in clear-sky regions but secondary in cloudy areas. Figure 8b shows changes in the reflected shortwave radiation (RSR) at TOA between the two assimilations. The differences in RSR are mainly caused by the changes in cloud coverage. Except for the polar regions, clouds are brighter than the surface underneath, that is, clouds have higher albedo than the surface. Thus the positive (negative) differences in RSR coexist with the positive (negative) differences in the cloud amount. Large differences found in the SH midlatitudes are associated with large solar irradiance in the summer hemisphere.

6. Discussion and conclusions

The assimilation experiment with the inclusion of the TOVS retrieved humidity has shown a large impact of the TOVS humidity on the assimilated humidity fields. It has been demonstrated that the impact results from direct and indirect effects. The direct effect is the analysis increment introduced by the humidity data. The

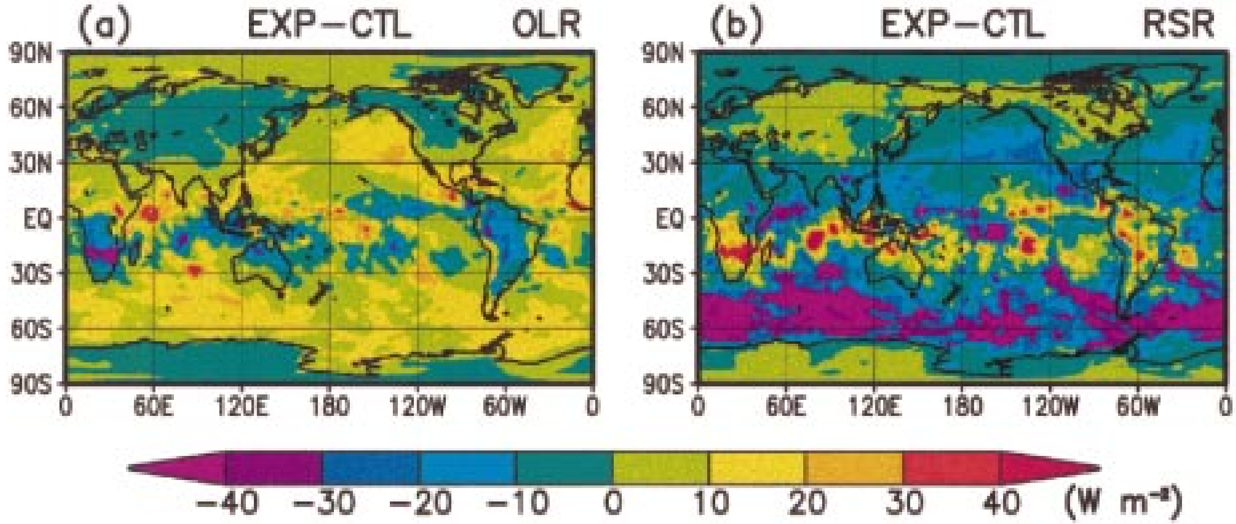

FIG. 8. Differences in (a) outgoing longwave radiation and (b) reflected shortwave radiation at TOA between EXP and CTL.

direct effect draws the assimilated humidity toward the observation. The GEOS-2 data assimilation system uses the TOVS data very effectively in terms of the direct effect. The indirect effect is realized through the interactions of humidity with physical processes, mainly with moist convection. The direct effect is dominant in the lower and middle troposphere while the indirect effect is more important than the direct effect in the tropical upper troposphere.

Due to the complicated nature of the interactions between humidity and physical processes, the indirect effect does not necessarily act in a way to draw an assimilation to humidity data. In the assimilation presented in this paper, the indirect effect is often opposite to the direct effect. In most regions along the ITCZ, deep convection is enhanced when the TOVS humidity is included. Due to the strong moistening effect of tropical deep convection (Chen et al. 1999), enhanced convection increases upper-tropospheric humidity. The moistening impact from enhanced convection is dominant over the negative forcing from the direct effect for the upper troposphere. This explains the inconsistency that the inclusion of the TOVS humidity data gives a wetter upper troposphere in southern Africa, South America, and some other tropical areas even though the TOVS upper-tropospheric humidity is significantly drier than the control assimilation.

The strong interactions between humidity and physical processes are also shown in the precipitation, cloud amount, and radiation fields. There are large changes in those fields when the TOVS humidity is included in the assimilation. The changes over most regions give an indication of deterioration compared with available independent observations, even though the humidity fields are better assimilated in the lower and middle troposphere. The lack of improvement on those physical fields is consistent with the unfavorable impact on upper-tropospheric humidity.

The unfavorable interactions between the TOVS humidity and the GEOS-2 physical parameterizations could result from either poor quality of the vertical structure of the TOVS humidity or deficiencies in the parameterizations. The good agreement of the TOVS TPW with the SSM/I TPW does not mean good quality of the vertical structure of the TOVS retrieval. However, comparisons of the TOVS retrieval with the ECMWF reanalysis (Gilbson et al. 1997) and historical rawinsonde data (Oort 1983) show that the vertical structure of the TOVS retrieval is more consistent with those datasets than the GEOS-2 control assimilation. Thus, the unfavorable interactions suggest that retuning of physical parameterizations is necessary for full use of the new data. The present GEOS-2 physical parameterizations have been tuned largely for optimal climate simulations with the GEOS-2 GCM. In standard GEOS assimilations the input humidity data is only from rawinsonde observations. It has been shown that there are unfavorable interactions between input data and moist convection in the GEOS-1 system, which unfavorably affect precipitation, clouds, radiation, and upper-tropospheric humidity (Molod et al. 1996; Chen et al. 1998). The moist convection in GEOS-2 is basically the same as in GEOS-1 (Moorthi and Suarez 1992). The unfavorable interactions exist in GEOS-2, though, to a less degree.

The TOVS humidity data is much greater in volume than rawinsonde data, especially in the Tropics. This could mean stronger interactions expected between the TOVS data and moist convection. Emerging evidence clearly indicates that tuning of physical parameterizations explicitly in the data assimilation mode is necessary for development of an optimal data assimilation system. Also, compared with tuning in the model simulation mode, tuning in the assimilation mode is more constrained by observations in direct and indirect ways. This means tuning in the assimilation mode is more data driven. We have a plan for in-depth studies of tuning the GEOS physical parameterizations explicitly for data assimilations.

The DAO has also been developing a one-dimensional variational analysis scheme to assimilate the TOVS humidity information (radiances) into the GEOS DAS (Joiner and Rokke 1998). The 1DVAR will be interactive, meaning that it will use forecasts from the same assimilation system as a background. This may give an improved assimilation of the TOVS humidity information. The TOVS Pathfinder dataset was designed to be a self-contained climate dataset. The tuning in the retrieval that has been applied to the Pathfinder dataset may not be optimal for data assimilations. It is hoped that the combination of the 1DVAR with model physics tuning in the assimilation mode will improve the GEOS assimilations of humidity and related physical fields.

Acknowledgments. We are grateful to Joel Susskind and Paul Piraino for assistance with the TOVS humidity data, Jing Guo, Yelena Kondratyeva, and David Lamich for assistance in running the GEOS-2 system, and Steve Cohn, Dick Dee, Arthur Hou, Siegfried Schubert, and Arlindo da Silva for helpful discussions. We also thank two anonymous reviewers for their helpful comments. This research was supported by the NASA EOS Interdisciplinary Project.

REFERENCES

Arakawa, A., and W. H. Schubert, 1974: Interaction of a cumulus cloud ensemble with the large-scale environment. Part I. *J. Atmos. Sci.,* **31,** 671–701.

Bloom, S. C., L. L. Takacs, A. M. da Silva, and D. Ledvina, 1996: Data assimilation using incremental analysis updates. *Mon. Wea. Rev.,* **124,** 1256–1271.

Cess, R. D., and Coauthors, 1990: Intercomparison and interpretation of climate feedback processes in 19 atmospheric general circulation models. *J. Geophys. Res.,* **95,** 16 601–16 615.

Chen, M., R. B. Rood, and W. G. Read, 1998: Upper tropospheric water vapor from GEOS reanalysis and UARS MLS observation. *J. Geophys. Res.,* **103,** 19 587–19 594.

——, ——, and ——, 1999: Seasonal variations of upper tropospheric water vapor and high clouds observed from satellites. *J. Geophys. Res.,* **104,** 6193–6197.

Chou, M.-D., 1992: A solar radiation model for use in climate studies. *J. Atmos. Sci.,* **49,** 762–772.

——, and M. J. Suarez, 1994: An efficient thermal infrared radiation parameterization for use in general circulation models. NASA Tech. Memo. 104606, Vol. 3, 85 pp.

Courtier, P., and Coauthors, 1998: The ECMWF implementation of three dimensional variational assimilation (3D-Var). Part I: Formulation. *Quart. J. Roy. Meteor. Soc.,* **124,** 1783–1807.

DAO, 1996: Algorithm theoretical basis document for Goddard Earth Observing System Data Assimilation System (GEOS DAS) with a focus on version 2. Data Assimilation Office, NASA's Goddard Space Flight Center, 310 pp.

Elliot, W. P., and D. J. Gaffen, 1991: On the utility of radiosonde humidity archives for climate studies. *Bull. Amer. Meteor. Soc.,* **72,** 1507–1520.

Eyre, J. R., G. A. Kelly, A. P. McNally, E. Andersson, and A. Persson, 1993: Assimilation of TOVS radiance information through one-dimensional variational analysis. *Quart. J. Roy. Meteor. Soc.,* **119,** 1427–1463.

Gilbson, J. K., P. Kallberg, S. Uppala, A. Hernandez, A. Nomura, and E. Serrano, 1997: ERA description. ECMWF Re-Analysis Project Report Series, 1, 72 pp. [Available from ECMWF, Shinfield Park, Reading, Berkshire RG2 9AX, United Kingdom.]

Helfand, H. M., and J. C. Labraga, 1988: Design of a nonsingular level 2.5 second-order closure model for the prediction of atmospheric turbulence. *J. Atmos. Sci.,* **45,** 113–132.

Huffman, G. J., and Coauthors, 1997: The Global Precipitation Climatology Project (GPCP) combined precipitation datasets. *Bull. Amer. Meteor. Soc.,* **78,** 5–20.

Joiner, J., and A. M. da Silva, 1998: Efficient methods to assimilate remotely sensed data based on information content. *Quart. J. Roy. Meteor. Soc.,* **124,** 1669–1694.

Kalnay, E., and Coauthors, 1996: The NCEP/NCAR 40-Year Reanalysis Project. *Bull. Amer. Meteor. Soc.,* **77,** 437–471.

Kousky, V. E., 1993: The global climate of December 1991–February 1992: Mature-phase warm (ENSO) episode conditions develop. *J. Climate,* **6,** 1639–1655.

McNally, A. P., and M. Vesperini, 1996: Variational analysis of humidity information from TOVS radiances. *Quart. J. Roy. Meteor. Soc.,* **122,** 1521–1544.

Molod, A., H. M. Helfand, and L. L. Takacs, 1996: The climate of the GEOS-1 GCM and its impact on the GEOS-1 data assimilation system. *J. Climate,* **9,** 764–785.

Moorthi, S., and M. J. Suarez, 1992: Relaxed Arakawa–Schubert: A parameterization of moist convection for general circulation models. *Mon. Wea. Rev.,* **120,** 978–1002.

Oort, A. H., 1983: Global atmospheric circulation statistics, 1958–1973. NOAA Prof. Paper 14, 180 pp.

Parrish, D. F., and J. C. Derber, 1992: The National Meteorological Center's statistical spectral interpolation analysis system. *Mon. Wea. Rev.,* **109,** 1747–1763.

Pfaendtner, J., S. Bloom, D. Lamich, M. Seablom, M. Sienkiewicz, J. Stobie, and A. da Silva, 1995: Documentation of the Goddard Earth Observing System (GEOS) data assimilation system-version 1. NASA Tech. Memo. 104606, Vol. 4, 44 pp.

Read, W. G., J. W. Waters, D. A. Flower, L. Froidevaux, R. F. Jarnot, D. L. Hartmann, R. S. Harwood, and R. B. Rood, 1995: Upper tropospheric water vapor from UARS MLS. *Bull. Amer. Meteor. Soc.,* **76,** 2381–2389.

Reuter, D., J. Susskind, and A. Pursch, 1988: First guess dependence of a physically based set of temperature humidity retrievals from HIRS2/MSU data. *J. Atmos. Oceanic Technol.,* **5,** 70–83.

Rind, D., E.-W. Chiou, W. Chu, S. Oltmans, J. Lerner, J. Larsen, M. P. McCormick, and L. McMaster, 1993: Overview of the stratospheric aerosol and gas experiment II water vapor observations: Method, validation, and data characteristics. *J. Geophys. Res.,* **98,** 4835–4856.

Rossow, W. B., and R. A. Schiffer, 1991: ISCCP cloud data products. *Bull. Amer. Meteor. Soc.,* **72,** 2–20.

Schmetz, J., and O. M. Turpeinen, 1988: Estimation of the upper tropospheric relative humidity field from METEOSAT water vapor image data. *J. Appl. Meteor.,* **27,** 889–899.

Schubert, S. D., and R. B. Rood, 1995: Proceedings of the Workshop on the GEOS-1 Five-Year Assimilation. NASA Tech. Memo. 104606, Vol. 7, 201 pp.

——, ——, and J. Pfaendtner, 1993: An assimilated dataset for earth science applications. *Bull. Amer. Meteor. Soc.,* **74,** 2331–2342.

——, and Coauthors, 1995: A multiyear assimilation with the GEOS-1 system: Overview and results. NASA Tech. Memo. 104606, Vol. 6, 183 pp.

Slingo, J. M., 1987: The development and verification of a cloud prediction scheme for the ECMWF model. *Quart. J. Roy. Meteor. Soc.,* **113,** 899–927.

Smith, W. L., H. M. Woolf, C. M. Hayden, D. Q. Wark, and L. M.

McMillin, 1979: The TIROS-N operational vertical sounder. *Bull. Amer. Meteor. Soc.,* **60,** 1177–1187.

Starr, D. O'C., and S. H. Melfi, 1991: The role of water vapor in climate: A strategic research plan for the proposed GEWEX Water Vapor Project (GVaP). NASA Conf. Publ. 3120, 50 pp.

Suarez, M. J., and L. L. Takacs, 1995: Documentation of the Aries/GEOS dynamical core: Version 2. NASA Tech. Memo. 104606, Vol. 5, 45 pp.

Sud, Y. C., and A. Molod, 1988: The roles of dry convection, cloud–radiation feedback processes and the influence of recent improvements in the parameterization of convection in the GLA GCM. *Mon. Wea. Rev.,* **116,** 2366–2387.

Sun, D. Z., and I. M. Held, 1996: A comparison of modeled and observed relationships between international variations of water vapor and temperature. *J. Climate,* **9,** 665–675.

Susskind, J., J. Rosenfield, D. Reuter, and M. T. Chahine, 1984: Remote sensing of weather and climate parameters from HIRS2/MSU on *TIROS-N. J. Geophys. Res.,* **89,** 467–469.

——, P. Piraino, L. Rokke, L. Iredell, and A. Mehta, 1997: Characteristics of the TOVS Pathfinder Path A dataset. *Bull. Amer. Meteor. Soc.,* **78,** 1449–1472.

Takacs, L. L., A. Molod, and T. Wang, 1994: Documentation of the Goddard Earth Observing System (GEOS) general circulation model-version 1. NASA Tech. Memo. 104606, Vol. 1, 100 pp.

Wentz, F., 1994: User's manual, SSM/I geophysical tapes. Remote Sensing Systems, 11 pp.

Zhou, J., Y. C. Sud, and K.-M. Lau, 1996: Impact of orographically induced gravity wave drag in the GLA GCM. *Quart. J. Roy. Meteor. Soc.,* **122,** 903–927.